



A New Sample of Mid-Infrared Bright, Long-Period Mira Variables
from the MACHO Galactic Bulge Fields

Klaus Bernhard^{1,3}, Stefan Uttenthaler², Stefan Hümerich^{1,3}

1) Bundesdeutsche Arbeitsgemeinschaft für Veränderliche Sterne e.V. (BAV)

2) Kuffner Observatory, Johann Staud-Straße 10, 1160 Wien, Austria

3) American Association of Variable Star Observers (AAVSO)

September 2016

Abstract: *Mid-infrared bright objects in the direction of the Galactic Bulge were investigated using time series photometry from the MACHO data archive, which led to the discovery of a large number of long-period variables. Among these, a total of 192 bona-fide Mira variables was identified, which – to the best of our knowledge – are reported here for the first time. Together with the results from our previous investigations, we thereby bring the number of Mira variables found in the MACHO Galactic Bulge fields to a new total of 1286 stars. Light curves, folded light curves and summary data for all new Mira variables are presented and their properties in colour-colour, period-colour and period-magnitude space are investigated. In agreement with our expectations, the present sample of mid-infrared bright objects is composed mostly of luminous, long-period variables.*

1. Introduction

Mira stars, named after their bright prototype Mira ('the wonderful', α Ceti), are radially pulsating variables exhibiting large photometric amplitudes and periods on the order of $80 \lesssim P(d) \lesssim 1000$, although stars with longer periods of up to 2000 days exist [1]. By definition, Mira stars show amplitudes of $\Delta V \geq 2.5$ mag [2], although this cut-off is to some extent arbitrary and results in physically similar stars being classified as semi-regular variables (GCVS-type SRA). Observed light amplitudes in the infrared are much smaller (e.g. $\Delta I \geq 0.8$ or 0.9 mag; $\Delta K \geq 0.4$ mag [3]).

Miras are low- and intermediate-mass stars in an advanced, short-lived ($\sim 2 \times 10^5$ years) state and populate the tip of the asymptotic giant branch (AGB) [4]. They are late-type stars with spectra indicative of strong molecular absorption features (e.g. TiO, ZrO, CN) and emission lines that result from pulsation-related shock waves. Thus, they are found at spectral types Me (oxygen-rich atmosphere), Ce (carbon-rich atmosphere), or, more rarely, Se (intermediate) [3]. The Mira phase is characterised by heavy mass loss, which is why Miras often show considerable circumstellar extinction because of thick dust shells (e.g. [5]). This holds true especially for the longer-period objects.

Mira variables have been shown to follow a distinct period luminosity relation [6]. Because of their luminosity, they are important distance indicators and tools for investigating Galactic structure (e.g. [7]). It is therefore important to increase the sample size of known Mira variables. Our own efforts

in this respect [8,9,10] have led to the identification of 1094 Mira variables in the Massive Compact Halo Object (MACHO) project data archive.

In the present investigation, we report on the discovery of an additional 192 Mira variables in the MACHO data archive that have been found by a different methodological approach. Observations and target selection are described in Section 2, data are analysed in Section 3. Results are presented and discussed in Section 4, and we conclude in Section 5.

2. Observations and Target Selection

2.1 The Massive Compact Halo Object (MACHO) Project

Aim of the MACHO Project was the search for dark matter in the form of massive compact halo objects, so called 'MACHOs'. To this end, millions of stars were monitored in the Magellanic Clouds and the Galactic Bulge in order to search for gravitational microlensing events caused by the – otherwise invisible – MACHOs [11]. As a by-product, thousands of variable stars were discovered in the resulting photometric data.

Observations were carried out between 1992 and 2000 with the 1.27m Great Melbourne Telescope situated at Mount Stromlo in Australia. Using a dichroic beam-splitter, all observations were taken simultaneously through the non-standard MACHO blue filter ($\sim 4500\text{-}6300 \text{ \AA}$; hereafter MACHO *B*-band) and MACHO red filter ($\sim 6300\text{-}7600 \text{ \AA}$; hereafter MACHO *R*-band) with a combination of eight $2048^*\!2048$ CCD cameras [12]. For more information on the MACHO project, the reader is referred to [11,12]. MACHO observations are available online through the MACHO Project data archive¹.

2.2 Target Selection

In our previous searches for Mira variables in the MACHO data archive, objects whose MACHO *R*-band light curves show a larger deviation than that of other stars of similar magnitude were selected and visually inspected in order to find suitable candidates. For the present investigation, a different methodological approach was taken. Mid-infrared bright objects in the direction of the Galactic Bulge² were chosen using observations from the Wide-field Infrared Survey Explorer (WISE), which surveyed the whole sky in the four infrared bands *W1*, *W2*, *W3*, and *W4*, which are centered at 3.4, 4.6, 12, and 22 μm , respectively [13]. Only objects with $W4 \leq 4$ mag were selected for the construction of an initial sample of candidate variable stars. This cut-off was imposed because these *W4*-bright objects appear as a general 'nuisance' in studies of star-formation regions towards the Galactic bulge (J. Alves, private communication). We also expect that with this cut-off we can identify objects with a clear shell signal that are likely to correspond to dust-veiled AGB stars.

3. Data Analysis

Light curves of our candidate stars were downloaded from the MACHO data archive and MACHO instrumental magnitudes were transformed on to the Kron-Cousins system by using equation (2) of [12]. The light curves were visually inspected, which led to the discovery of 1169 clearly variable objects (mostly large amplitude semi-regular and Mira variables). Doubtful cases and stars whose variability is obviously caused by instrumental artifacts (mostly blending issues) were rejected.

In order to separate Miras from semi-regular variables, stars with an amplitude > 2 mag (R_C) were selected (cf. [9,10]). Objects exhibiting significant changes in amplitude, mean magnitude and / or period suggesting semi-regularity were subsequently rejected. The sample of Mira variables was cross-matched with the 2MASS Catalog [15], from which we derived astrometric positions and

¹ <http://macho.anu.edu.au/>

² Centre coordinates of the MACHO Galactic Bulge fields are found at http://macho.nci.org.au/Macho_fields.html.

near-infrared color indices. Each object was checked against the VizieR service [16] and the AAVSO International Variable Star Index (VSX; [17]) for any information in variability catalogues about the existence of a Mira star at the given position. Known Mira variables were dropped from the sample. In total, we identified 192 new bona-fide Mira variables.

4. Results

4.1 The New Sample

Following the methodology outlined above, a total of 192 Mira variables in the direction of the Galactic Bulge were found in the MACHO data archive. To the best of our knowledge, these Miras are reported here for the first time. Light curves, folded light curves and summary data for all new Mira variables are presented in the Appendix (Table 1 and Figure 6).

4.2 Statistical Analyses

In the following subsections, statistical properties of the present sample of mid-infrared bright Mira variables ($N = 192$) are investigated and compared to the properties of the sample of Mira variables from the MACHO Galactic Bulge fields presented in [8,9,10] ($N = 1094$). For ease of use, the present sample is referred to in the following as the MIBR (**mid-infrared bright**) sample.

4.2.1 Period Distribution

A comparison of the period distribution of the MIBR sample ($N = 192$) with the sample of Mira variables presented in [8,9,10] ($N = 1094$) is shown in Figure 1 (cf. also Figure 6 in [10]). It becomes obvious that the MIBR sample contains considerably more Miras of longer period, particularly in the range $350 \leq P(d) \leq 500$. Several Miras of the sample show periods close to one year, which results in poor phase coverage that may pose problematic for standard period search algorithms. However, in our previous searches for Mira variables in the MACHO database [8,9,10], suitable candidates were chosen by visual inspection only. We therefore expect no bias in the discovery of variables with periods close to one year in our previous samples and are confident that the excess of long-period Miras in the MIBR sample is significant and an intrinsic characteristic of the sample.

An excess of long-period Miras is to be expected as the present sample is exclusively made up of mid-infrared bright stars with $W4 \leq 4$ mag (cf. Section 2.2), which correspond to highly reddened objects. It is a well-known fact that long-period ($\log(P) \gtrsim 2.5$; cf. e.g. [19]) Miras are prone to exhibiting considerable colour excess due to circumstellar dust shells [19]; thus, very red Miras are usually also long-period Miras. This phenomenon is also obvious in the period-colour diagram presented below (cf. Figure 3).

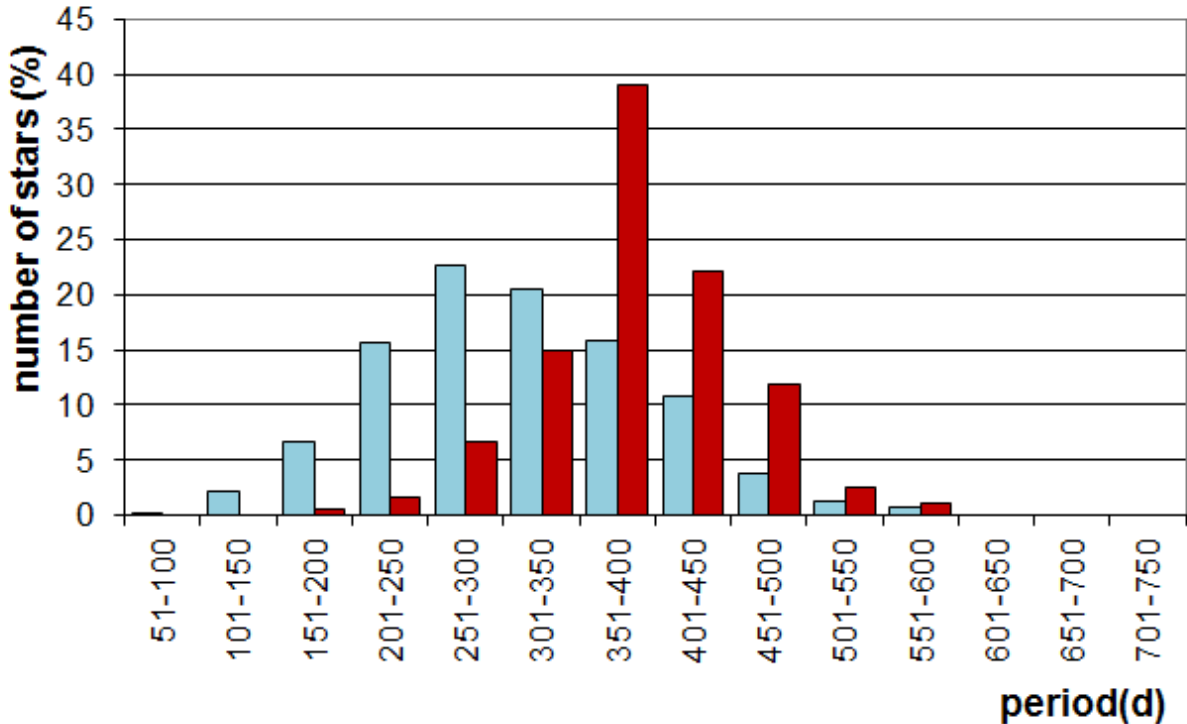


Figure 1 – Period distribution of Mira variables found in the MACHO Galactic Bulge fields, based on the MIBR sample (red; $N = 192$) and the samples presented in [8,9,10] (blue, $N = 1094$).

4.2.2 Colour-Magnitude Diagram

A colour-magnitude diagram, based on 2MASS photometry, is presented in Figure 2. 2MASS observations generally consist of six consecutive exposures for a total integration time of 7.8 seconds [15]. Most objects were visited only once during the course of the survey, which also applies to the Miras of the MIBR sample. Some scatter, therefore, would be expected due to the unknown pulsational phase at which the 2MASS observations were taken.

However, the observed amplitudes of Mira variables in the K_s -band are relatively small (cf. Section 1), and the scatter introduced by the single-epoch measurements is very small in comparison to the distribution of brightness in Figure 2. This also holds true for the $(H-K_s)$ colour index derived from 2MASS and employed in Figure 3. Thus, the scatter introduced by the single-epoch measurements is negligible in this context and does not preclude us from drawing conclusions from Figures 2 and 3.

Note the 'red tail' of Miras with $(H-K_s) \geq 1$ that extends to $(H-K_s) \sim 1.5$, which is present in both samples. The presence of this feature confirms the findings of [19] (cf. in particular their Figure 7) and is most obvious in the colour-magnitude diagram for the sample of Mira stars from the OGLE-III Catalog of Long-Period Variables (LPVs) in the Galactic Bulge [20], which is presented in Figure 7 of [10]. Apparently, Miras with $(H-K_s) \geq 1$ become fainter in the K_s -band with increasing $(H-K_s)$, which is likely caused by circumstellar extinction due to dust (e.g. [21]). As expected, the Miras of the MIBR sample are mostly situated at the red ($(H-K_s) \gtrsim 0.60$ mag) and bright ($K_s \lesssim 7.5$ mag) end of the 'main clump' of Mira variables in the diagram.

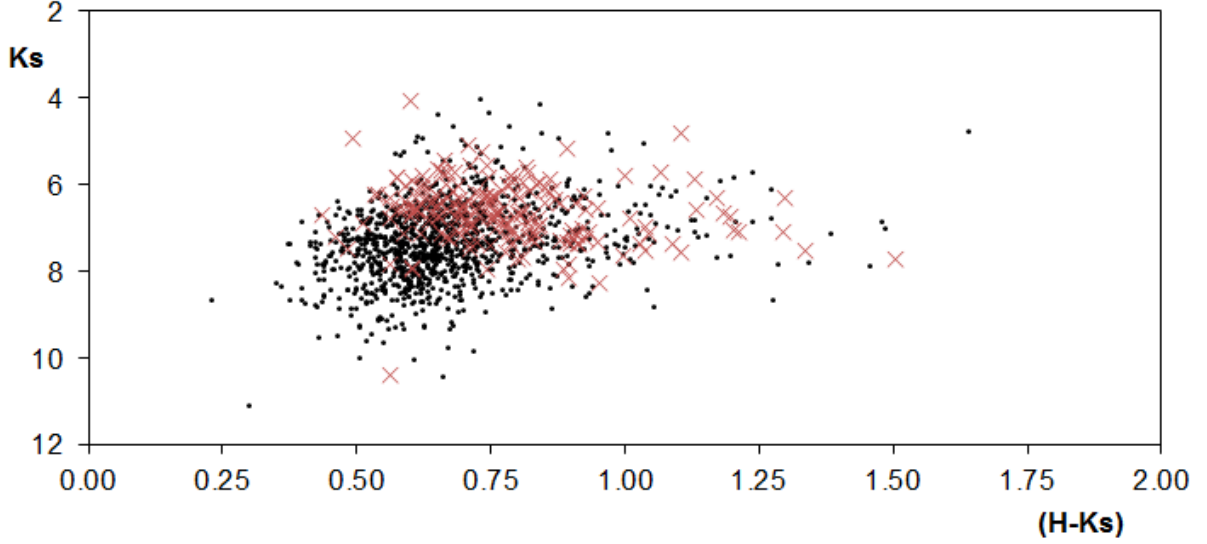


Figure 2 - 2MASS $(H-K_s)$ vs. K_s diagram, illustrating the positions of the Mira variables of the MIBR sample (red crosses; $N = 192$) and the samples presented in [8,9,10] (black dots, $N = 1094$).

4.2.3 Period-Colour Diagram

A period-colour diagram is given in Figure 3, which confirms that Miras of longer period have larger $(H-K_s)$ values and hence redder colours. This agrees with earlier findings from OGLE data [19, in particular their Fig. 10], where a significant increase or even a step in $(H-K_s)$ colour is reported at $\log(P) \sim 2.6$. This is likely caused by colour excess due to circumstellar dust that is observed for Miras with periods longer than this value (cf. Section 4.2.1 and [19]). The Miras of the MIBR sample are nearly exclusively found among the long-period objects with $\log(P) \gtrsim 2.5$.

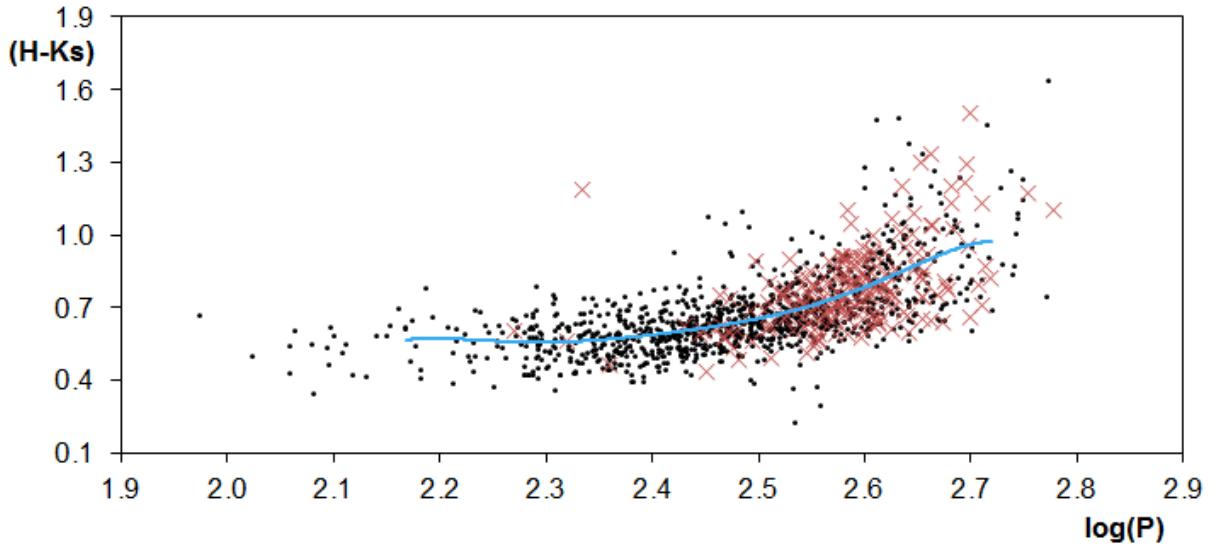


Figure 3 – $\log(P)$ vs. 2MASS $(H-K_s)$ diagram, illustrating the positions of the Mira variables of the MIBR sample (red crosses; $N = 192$) and the samples presented in [8,9,10] (black dots, $N = 1094$). The blue line indicates the moving average. Note the increase in $(H-K_s)$ colour at $\log(P) \sim 2.6$.

4.2.4 Period-Magnitude Diagram

Variable red giant stars occupy several well-known sequences in period-luminosity space [22]. Miras and Mira-like semi-regular variables occupy what is commonly referred to as sequence C and are well separated from semi-regular variables of smaller amplitude (like e.g. the so-called OSARG (**OGLE Small Amplitude Red Giant**) variables). We have investigated the distribution of the MACHO Mira samples in the near-infrared period-magnitude diagram, using 2MASS K_s photometry, which – for red giant stars in the Galactic Bulge – serves as a reasonable proxy for absolute magnitude (Figure 4). Again, as expected, the Miras of the MIBR sample are situated almost exclusively at the bright, long-period end.

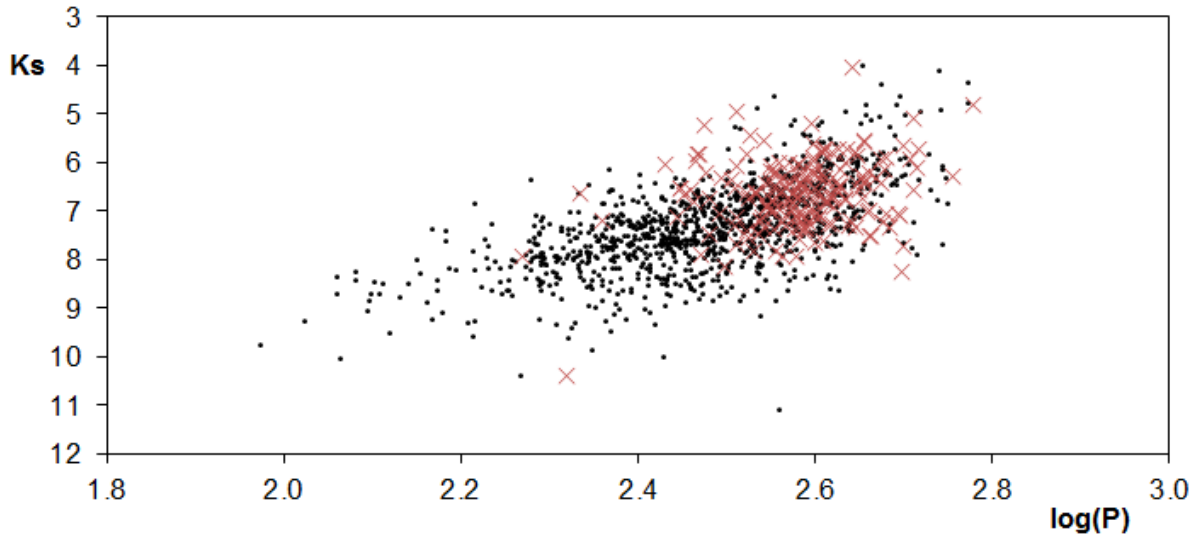


Figure 4 – $\log(P)$ vs. 2MASS K_s diagram, illustrating the positions of the Mira variables of the MIBR sample (red crosses; $N = 192$) and the samples presented in [8,9,10] (black dots, $N = 1094$).

Although there is considerable scatter due to reddening (line-of-sight extinction, circumstellar extinction), the general trend is clearly visible and our result is in excellent agreement with the findings in the literature (cf. e.g. [20], especially their Figure 5, and [22]).

At very strong circumstellar extinction, even the near-IR K_s band loses its power as luminosity indicator of red giant stars. In order to reduce the effects of extinction, we have constructed a period-magnitude diagram for the MIBR sample that is based on the reddening-independent Wesenheit index W_{JK} (e.g. [20]), the result of which is shown in Figure 5. The Wesenheit W_{JK} index is defined as

$$W_{JK} = K - 0.686(J - K). \quad (1)$$

This helps to reduce the scatter and narrow down the sequence, although some clear outliers remain that have a severe effect on the linear regression fit. Nevertheless, sequence C is clearly visible in the plot.

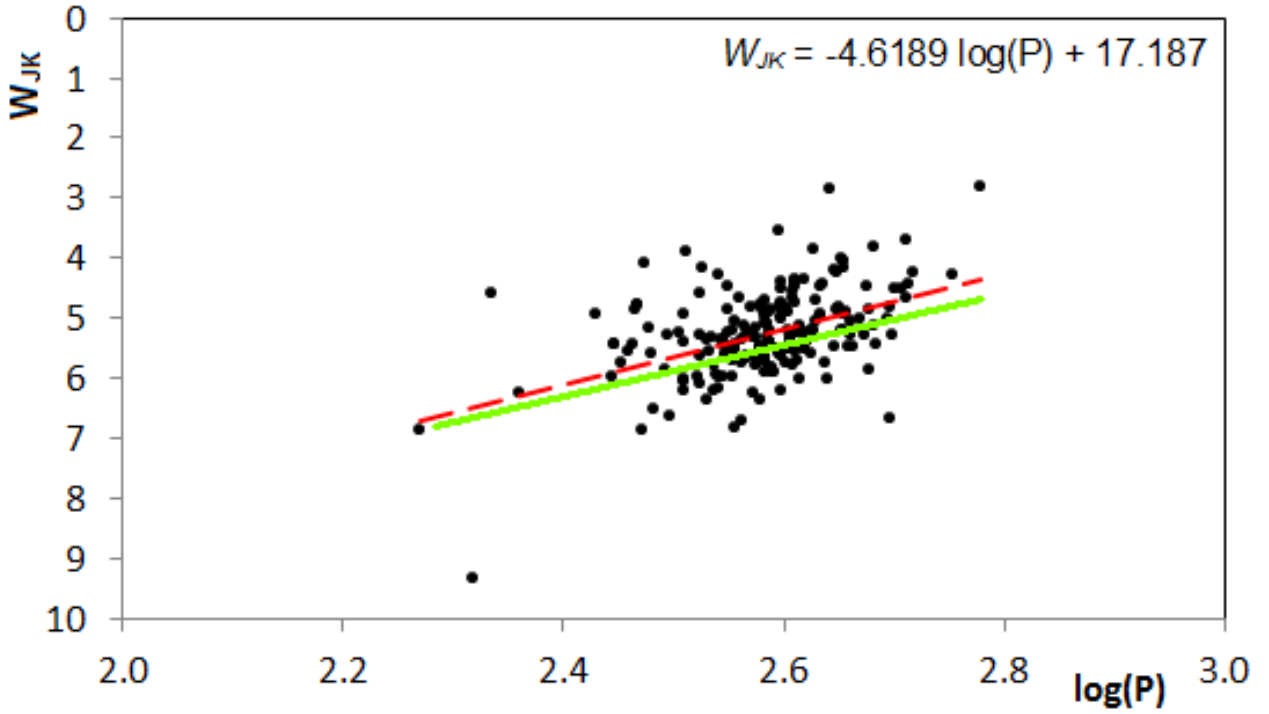


Figure 5 – $\log(P)$ vs. W_{JK} diagram, illustrating the positions of the Mira variables of the MIBR sample (red crosses; $N = 192$). The dashed red line is a linear fit to the data; the solution is reproduced in the upper right of the diagram. The green line roughly indicates the position of sequence C based on an approximate fit to the data in Fig. 5 of [20].

5. Conclusion

We have investigated mid-infrared bright objects (WISE $W4 \leq 4$ mag) in the direction of the Galactic Bulge using time series photometry from the MACHO data archive, which led to the discovery of a large number of long-period variables. A total of 192 bona-fide Mira variables was found, which have not been included in existing variability catalogues, and which are – to the best of our knowledge – announced here for the first time. Together with the results from our previous investigations [8,9,10], we bring the number of Mira variables found in the MACHO Galactic Bulge fields to a new total of 1286 stars.

We present light curves, folded light curves and summary data for all new Mira variables and investigate their properties in colour-colour, period-colour and period-magnitude space. As expected, the present sample of mid-infrared bright objects is composed mostly of luminous, long-period Miras.

Acknowledgements

We thank Prof. João Alves (University of Vienna) for discussions on mid-infrared bright objects in the direction of the Pipe Nebula which provided the stimulus that instigated this research. This paper utilizes public domain data obtained by the MACHO Project, jointly funded by the US Department of Energy through the University of California, Lawrence Livermore National Laboratory under contract No. W-7405-Eng-48, by the National Science Foundation through the Center for Particle Astrophysics of the University of California under cooperative agreement AST-8809616, and by the Mount Stromlo and Siding Spring Observatory, part of the Australian National University. This research has also made use of the SIMBAD and VizieR databases operated at the Centre de Données Astronomiques (Strasbourg) in France. Furthermore, data products from the Two Micron All Sky Survey were employed, which is a joint project of the University of Massachusetts and the Infrared Processing and Analysis Center/California Institute of Technology, funded by the National Aeronautics and Space Administration and the National Science Foundation.

References

- [1] Whitelock, P., Menzies, J., Feast, M., et al. 1994, MNRAS, 267, 711
- [2] Samus, N. N., Durlevich, O. V., Kazarovets, E. V., et al. 2007-2016, General Catalogue of Variable Stars, VizieR On-line Catalog (<http://cdsarc.u-strasbg.fr/viz-bin/Cat?B/gcvs>)
- [3] Whitelock, P. 2012, Ap&SS, 341, 123
- [4] Whitelock, P., Marang, F., Feast, M. 2000, MNRAS, 319, 728
- [5] Ita, Y., Matsunaga, N. 2011, MNRAS, 412, 2345
- [6] Whitelock, P., Feast, M., van Leeuwen, F. 2008, MNRAS, 386, 313
- [7] Catchpole, R., Whitelock, P., Feast, M. 2016, MNRAS, 455, 2216
- [8] Bernhard, K. 2011, PZP, 11, 12
- [9] Huemmerich, S., Bernhard, K. 2012, OEJV, 149, 1
- [10] Bernhard, K., Huemmerich, S., 2013, OEJV, 159, 1
- [11] Alcock, C., Allsman, R., Alves, D., et al. 1997, ApJ, 486, 697
- [12] Alcock, C., Allsman, R., Alves, D., et al. 1999, PASP, 111, 1539
- [13] Wright, E.L., Eisenhardt, P.R.M., Mainzer, A.K., et al. 2010, AJ, 140, 1868
- [14] Lenz, P., Breger, M. 2005, CoAst, 146, 53
- [15] Skrutskie, M. F., Cutri, R. M., Stiening, R., et al. 2006, AJ, 131, 1163
- [16] Ochsenbein, F., Bauer, P., Marcout, J. 2000, A&AS, 143, 23 (VizieR)
- [17] Watson, C. L. 2006, SASS, 25, 47 (AAVSO International Variable Star Index)
- [18] Zijlstra, A., Bedding, T. 2002, JAVSO, 31, 2
- [19] Matsunaga, N., Fukushi, H., Nakada, Y. 2005, MNRAS, 364, 117
- [20] Soszyński, I., Udalski, A., Szymański, M. K., et al. 2013, AcA, 63, 21
- [21] Fraser, O. J. 2008, PhDT, Proquest / UMI, AAT 3328397
- [22] Wood, P. R., Alcock, C., Allsman, R. A., et al. 1999, in IAU Symp. 191, Asymptotic Giant Branch Stars, ed. T. Le Bertre, A. Lebre, & C. Waelkens (Cambridge: Cambridge Univ. Press), 151

Appendix

Table 1: Essential data for the new sample of 192 Mira variables identified in the MACHO data archive. Positional information and ($J-K_s$) indices were derived from the 2MASS catalogue.

MACHO ID	RA (J2000)	DEC (J2000)	2MASS ID	$J-K_s$	P(d)	Epoch (max)	Max (Rc)	Min (Rc)
403.47547.34	17 54 56.370	-29 48 33.53	17545637-2948335	1.639	292	2451041	11.2	15.2
402.47682.580	17 55 25.487	-28 48 10.67	17552548-2848106	2.046	382	2451220	<14.2	17.6
402.47676.192	17 55 33.638	-29 11 30.60	17553363-2911305	1.837	380	2451241	13.2	17.0
402.47741.111	17 55 46.512	-28 51 10.54	17554651-2851105	2.154	314	2451432	13.1	18.0
402.47745.888	17 55 49.681	-28 35 14.71	17554968-2835147	2.650	406	2450174	16.4	19.7
402.47864.438	17 56 21.990	-28 39 59.89	17562192-2839598	1.825	412	2450547	14.8	17.6
403.47853.1588	17 56 26.667	-29 25 41.71	17562666-2925417	2.520	387	2449976	15.0	17.8
401.47877.236	17 56 26.781	-27 50 12.92	17562678-2750129	2.449	369	2451220	16.0	19.6
403.47906.1195	17 56 37.073	-29 52 33.25	17563707-2952332	2.191	417	2450907	15.0	18.9
403.47909.1283	17 56 40.307	-29 40 37.18	17564030-2940371	2.264	450	2449942	14.4	16.7
401.48053.1848	17 57 09.327	-28 05 43.88	17570932-2805438	2.306	379	2450040	15.1	18.6
401.48050.561	17 57 09.307	-28 15 22.60	17570930-2815226	2.112	339	2451444	14.4	17.3
402.48099.17	17 57 31.212	-29 00 04.53	17573121-2900045	2.017	452	2450182	13.1	15.4
402.48096.271	17 57 32.987	-29 11 00.12	17573298-2911001	2.270	397	2451463	14.8	17.7
118.18270.862	17 58 56.439	-30 05 10.29	17585643-3005102	2.024	475	2451326	14.2	17.8
118.18796.636	18 00 05.315	-29 43 28.64	18000531-2943286	1.741	352	2450646	12.7	16.7
176.18832.33	18 00 17.705	-27 17 36.55	18001770-2717365	1.954	363	2451344	14.0	16.4
118.18921.2024	18 00 32.809	-29 59 44.55	18003280-2959445	2.963	461	2450345	15.5	19.5
176.18955.1440	18 00 33.529	-27 47 05.09	18003352-2747050	2.506	382	2450534	15.6	19.5
176.19089.44	18 00 52.958	-27 30 19.14	18005295-2730191	2.260	452	2449816	13.0	18.1
176.19352.3590	18 01 16.258	-27 19 12.75	18011625-2719127	2.264	382	2450517	15.2	18.6
176.19481.2463	18 01 41.482	-27 22 22.05	18014148-2722220	2.381	401	2451310	15.8	19.5
104.20384.163	18 03 50.474	-27 50 42.30	18035047-2750422	1.684	359	2449054	<12.9	18.0
120.21002.18	18 05 19.463	-29 56 51.69	18051946-2956516	1.586	360	2449061	11.8	15.8
120.21395.12	18 06 18.306	-29 44 11.89	18061830-2944118	1.055	374	2450259	13.1	>15.7
121.21382.110	18 06 23.626	-30 36 21.13	18062362-3036211	1.630	405	2451305	12.0	17.0
179.21577.71	18 06 37.262	-26 19 25.07	18063726-2619250	1.954	342	2450505	13.5	16.3
121.21517.25	18 06 43.807	-30 18 38.00	18064380-3018380	1.723	410	2449156	13.0	15.3
124.21640.914	18 06 47.617	-30 47 15.72	18064761-3047157	1.832	408	2449109	12.1	16.8
179.21712.731	18 06 51.813	-25 59 21.91	18065181-2559219	2.205	430	2451305	14.1	17.7
124.21632.42	18 06 51.930	-31 16 45.67	18065193-3116456	1.591	410	2450247	12.5	15.9
120.21784.522	18 07 07.436	-29 49 13.39	18070743-2949133	2.452	380	2450018	13.7	16.7
121.21777.223	18 07 09.804	-30 17 39.49	18070980-3017394	1.799	366	2450664	13.2	17.0
124.21894.182	18 07 24.097	-31 10 43.65	18072409-3110436	1.933	391	2449843	14.4	>17.8
120.21911.3312	18 07 33.449	-30 01 00.98	18073344-3001009	1.593	320	2449900	10.6	14.8
180.22499.1546	18 08 45.662	-25 27 45.86	18084566-2527458	2.270	412	2451251	15.8	18.8
121.22423.17	18 08 48.124	-30 31 45.03	18084812-3031450	1.617	324	2449105	11.7	15.7
110.22582.55	18 09 01.782	-28 35 48.48	18090178-2835484	1.843	336	2449843	11.8	17.5
121.22555.10	18 09 02.714	-30 26 14.82	18090271-3026148	1.763	438	2451384	10.5	14.2
178.22751.265	18 09 15.219	-26 01 03.54	18091521-2601035	2.560	446	2450273	15.1	18.3
110.22708.392	18 09 16.297	-28 53 02.57	18091629-2853025	2.130	395	2449988	14.0	18.3
127.22793.24	18 09 44.504	-31 53 52.23	18094450-3153522	2.007	389	2449153	13.1	16.8
180.23019.926	18 10 02.169	-25 31 12.57	18100216-2531125	2.699	443	2450601	15.8	20.0
180.23151.26	18 10 12.393	-25 20 05.55	18101239-2520055	1.730	366	2450942	12.6	>17.0
125.23200.58	18 10 33.182	-30 44 33.30	18103318-3044333	1.365	351	2450715	10.9	15.6
102.23380.29	18 10 56.783	-27 26 58.29	18105678-2726582	1.614	269	2449109	12.5	18.0
122.23464.38	18 11 04.391	-30 31 12.28	18110439-3031122	1.693	459	2450657	13.2	15.6
167.23649.338	18 11 30.270	-26 50 25.20	18113026-2650252	1.807	323	2449179	12.7	16.3
178.23785.139	18 11 41.056	-26 25 36.51	18114105-2625365	1.736	375	2449950	12.9	16.7
116.23736.60	18 11 43.594	-29 43 30.48	18114359-2943304	2.140	522	2450580	12.4	15.5
167.23774.170	18 11 44.238	-27 09 24.44	18114423-2709244	1.857	387	2451281	<12.8	15.9
122.23730.28	18 11 44.212	-30 06 30.15	18114421-3006301	2.009	402	2449154	13.5	15.8
167.23776.107	18 11 48.762	-27 01 32.15	18114876-2701321	1.920	355	2451361	13.6	>15.8
167.23776.677	18 11 53.409	-27 01 19.42	18115340-2701194	2.249	387	2451280	13.9	17.2
167.23905.62	18 12 01.280	-27 06 42.62	18120128-2706426	1.481	288	2451313	10.8	14.6
111.23878.37	18 12 05.619	-28 52 46.27	18120561-2852462	1.651	324	2451313	11.0	14.9
111.23873.16	18 12 08.983	-29 12 38.54	18120898-2912385	1.551	325	2451351	11.6	13.6
161.24051.211	18 12 13.207	-26 02 25.44	18121320-2602254	2.274	389	2449201	13.2	17.5
116.24126.2803	18 12 47.280	-29 39 59.43	18124728-2939594	2.047	333	2450932	13.7	17.2
167.24294.33	18 12 53.100	-27 08 05.99	18125309-2708059	1.655	354	2449005	<12.2	15.8
116.24255.712	18 12 55.466	-29 45 17.80	18125546-2945177	2.294	444	2449926	15.2	18.5
167.24426.144	18 13 11.870	-27 01 05.39	18131186-2701053	2.065	426	2450301	13.6	15.8
116.24392.970	18 13 17.421	-29 16 39.00	18131742-2916390	2.276	435	2449234	14.3	17.4
116.24392.1337	18 13 25.544	-29 16 07.94	18132554-2916079	1.943	384	2451250	<14.1	17.2
167.24559.794	18 13 43.036	-26 49 41.18	18134303-2649411	2.109	510	2449224	14.4	17.9
161.24825.451	18 14 02.530	-26 26 51.95	18140252-2626519	1.909	375	2450875	14.4	16.8

307.35039.28	18 14 27.622	-23 47 45.08	18142762-2347450	2.122	374	2450020	13.6	16.7
307.35035.93	18 14 27.787	-24 03 24.48	18142778-2403244	2.501	403	2449964	14.4	17.3
177.24974.49	18 14 29.950	-25 08 32.25	18142994-2508322	2.075	382	2450186	12.8	16.4
306.35055.307	18 14 32.511	-22 46 38.09	18143251-2246380	2.363	395	2451247	<14.1	18.5
306.35044.66	18 14 32.753	-23 27 40.24	18143275-2327402	1.986	417	2450943	14.4	18.2
307.35044.281	18 14 32.753	-23 27 40.24	18143275-2327402	1.986	417	2450527	14.4	18.2
177.24975.162	18 14 33.675	-25 04 21.14	18143367-2504211	2.310	408	2451220	13.9	17.0
161.25086.27	18 14 46.626	-26 21 23.13	18144662-2621231	1.520	293	2450643	11.1	14.8
162.25092.4373	18 14 47.374	-25 59 40.20	18144737-2559401	1.936	386	2450016	12.1	16.1
306.35220.158	18 14 49.579	-22 57 05.53	18144957-2257055	1.951	451	2450885	14.4	17.0
305.35409.346	18 14 54.724	-21 34 10.83	18145472-2134108	2.331	354	2450024	<14.9	18.2
307.35373.38	18 14 55.322	-23 56 13.37	18145532-2356133	2.141	380	2449892	14.3	17.0
306.35383.89	18 14 59.089	-23 17 32.84	18145908-2317328	1.960	334	2451089	<13.6	16.4
307.35373.337	18 15 08.104	-23 55 37.15	18150810-2355371	1.825	361	2450038	<14.0	16.8
161.25218.1431	18 15 08.941	-26 13 45.78	18150894-2613457	2.078	416	2451355	15.0	18.9
305.35571.2200	18 15 18.605	-21 56 46.40	18151860-2156463	2.923	600	2451231	16.0	20.7
305.35571.2	18 15 19.640	-21 55 31.18	18151964-2155311	1.811	380	2450665	12.9	15.8
168.25334.4601	18 15 23.370	-27 09 58.94	18152336-2709589	2.182	453	2450954	14.2	16.9
162.25341.218	18 15 26.484	-26 40 17.99	18152648-2640179	2.295	379	2450835	<13.8	16.3
162.25346.3115	18 15 26.897	-26 21 04.28	18152689-2621042	2.726	383	2449214	13.9	17.6
159.25486.509	18 15 40.334	-25 42 41.96	18154033-2542419	2.796	483	2450596	16.2	19.1
168.25462.4818	18 15 40.696	-27 18 47.64	18154069-2718476	2.787	514	2450305	15.8	20.5
306.35887.19	18 15 43.694	-23 17 21.02	18154369-2317210	1.681	278	2451276	12.8	15.7
306.35886.142	18 15 47.607	-23 19 58.36	18154760-2319583	2.021	514	2450705	12.8	16.4
148.25549.18	18 16 03.144	-30 11 05.51	18160314-3011055	1.590	395	2450200	12.2	>15.9
168.25595.4518	18 16 07.891	-27 05 31.82	18160789-2705318	1.714	298	2451025	11.6	14.1
304.36069.723	18 16 09.222	-22 20 06.34	18160922-2220063	3.296	497	2451387	17.9	20.7
162.25736.298	18 16 12.046	-26 21 12.02	18161204-2621120	2.468	459	2449104	16.0	21.5
304.36240.3389	18 16 19.901	-22 07 23.65	18161990-2207236	3.338	459	2450571	17.2	20.5
306.36229.168	18 16 27.221	-22 52 58.07	18162722-2252580	1.879	433	2450884	14.5	17.9
155.25788.48	18 16 31.518	-31 33 11.67	18163151-3133116	1.436	422	2450641	11.6	15.5
159.25873.271	18 16 31.678	-25 55 16.35	18163167-2555163	1.998	394	2450882	13.4	15.8
159.25873.42	18 16 33.287	-25 54 47.36	18163328-2554473	1.578	350	2450105	12.6	15.7
306.36388.17	18 16 35.649	-23 27 19.34	18163564-2327193	1.563	280	2451341	11.2	15.5
306.36398.31	18 16 37.263	-22 50 33.85	18163726-2250338	1.668	323	2449923	12.8	16.2
159.25880.24	18 16 41.343	-25 25 22.86	18164134-2525228	1.789	365	2449115	13.0	>16.3
152.25795.34	18 16 46.300	-31 04 52.74	18164630-3104527	1.685	396	2450623	12.5	>16.7
162.25992.77	18 16 50.900	-26 35 55.69	18165090-2635556	1.695	396	2450240	13.2	15.6
162.26122.17	18 17 08.790	-26 38 51.09	18170878-2638510	1.833	348	2449891	10.7	>13.3
159.26142.374	18 17 13.971	-25 16 58.36	18171397-2516583	2.029	353	2450050	<14.2	17.6
159.26133.30	18 17 14.354	-25 52 51.90	18171435-2552518	1.715	376	2450577	12.4	>16.0
148.26069.278	18 17 21.573	-30 11 07.97	18172157-3011079	2.155	324	2449888	13.8	17.6
159.26270.62	18 17 29.061	-25 26 22.79	18172906-2526227	1.906	407	2451291	12.5	15.9
168.26243.224	18 17 33.106	-27 14 48.52	18173310-2714485	2.495	406	2450909	14.6	17.2
309.36913.38	18 17 34.325	-22 04 44.67	18173432-2204446	2.400	518	2449919	14.3	16.5
168.26244.769	18 17 34.989	-27 11 09.98	18173498-2711099	2.841	480	2450666	15.9	19.5
168.26243.222	18 17 36.617	-27 14 54.66	18173661-2714546	1.769	396	2451331	12.9	16.7
311.36886.124	18 17 38.272	-23 52 19.41	18173827-2352194	1.761	452	2450617	13.6	15.6
159.26398.18	18 17 42.579	-25 34 27.67	18174257-2534276	2.053	345	2449085	<13.4	17.0
310.37068.189	18 17 46.105	-22 57 07.48	18174610-2257074	2.164	365	2449971	12.1	16.4
311.37052.34	18 17 47.594	-24 02 31.07	18174759-2402310	1.653	302	2451026	12.6	15.8
310.37062.2051	18 17 51.027	-23 22 37.44	18175102-2322374	2.978	494	2450640	15.5	19.4
159.26395.19	18 17 51.117	-25 43 47.84	18175111-2543478	1.613	335	2449827	11.6	15.6
309.37079.321	18 17 52.604	-22 13 10.51	18175260-2213105	2.356	442	2450973	12.9	17.7
308.37091.896	18 17 53.054	-21 25 00.44	18175305-2125004	3.001	480	2450222	17.1	20.6
309.37241.101	18 18 07.106	-22 38 04.59	18180710-2238045	1.828	344	2449775	<13.1	16.9
311.37219.401	18 18 07.710	-24 03 58.06	18180771-2403580	1.945	399	2451289	14.0	16.6
311.37225.69	18 18 13.858	-23 42 04.49	18181385-2342044	1.792	346	2449787	12.6	16.7
309.37413.667	18 18 20.084	-22 20 15.91	18182008-2220159	2.652	430	2450159	15.7	18.8
310.37400.99	18 18 22.842	-23 11 54.96	18182284-2311549	1.712	348	2449770	<12.9	16.6
148.26588.65	18 18 26.748	-30 12 43.81	18182674-3012438	1.881	423	2450577	14.0	16.7
308.37421.1264	18 18 29.231	-21 49 33.62	18182923-2149336	2.379	378	2450030	15.4	18.8
309.37411.685	18 18 30.771	-22 28 41.83	18183077-2228418	2.952	568	2450295	16.4	18.4
163.26649.58	18 18 31.640	-26 10 03.00	18183164-2610030	1.519	300	2449877	11.5	15.3
152.26706.50	18 18 40.928	-31 02 39.52	18184092-3102395	1.651	374	2450246	13.0	>15.7
308.37594.263	18 18 41.073	-21 30 47.42	18184107-2130474	2.387	444	2449931	15.9	18.7
152.26703.17	18 18 45.428	-31 13 01.79	18184542-3113017	1.677	501	2450974	11.7	16.0
148.26717.152	18 18 50.816	-30 19 33.11	18185081-3019331	1.895	467	2450671	12.2	15.4
163.26778.30	18 18 51.107	-26 14 22.19	18185110-2614221	2.111	387	2449225	13.4	16.4
311.37723.52	18 18 56.779	-24 04 19.62	18185677-2404196	1.712	384	2449933	13.6	15.6
308.37754.2956	18 19 01.968	-21 59 38.43	18190196-2159384	1.838	334	2451402	<12.6	15.8
160.26916.12	18 19 05.656	-25 41 03.57	18190565-2541035	1.955	400	2450682	11.2	15.1
309.37913.118	18 19 08.668	-22 35 32.22	18190866-2235322	2.275	396	2450016	13.6	16.6
160.27052.8	18 19 18.230	-25 16 25.10	18191822-2516251	1.786	364	2450203	12.3	>14.8
308.37927.53	18 19 19.688	-21 42 43.17	18191968-2142431	2.320	498	2449933	15.1	19.4

163.27039.1305	18 19 20.067	-26 09 08.93	18192006-2609089	1.876	358	2451090	<13.6	16.3
309.38080.54	18 19 26.324	-22 39 02.53	18192632-2239025	2.151	397	2449952	13.9	15.8
309.38082.94	18 19 29.969	-22 32 30.87	18192996-2232308	2.026	402	2449971	12.9	16.7
163.27032.2748	18 19 30.688	-26 37 23.72	18193068-2637237	1.622	356	2451384	12.3	16.6
309.38085.49	18 19 32.294	-22 19 04.32	18193229-2219043	1.781	340	2450110	12.3	16.4
310.38237.86	18 19 41.519	-23 25 30.15	18194151-2325301	1.678	360	2449775	12.2	16.1
308.38599.62	18 20 17.077	-21 42 22.94	18201707-2142229	2.126	397	2449970	14.9	18.2
160.27441.217	18 20 17.758	-25 23 28.12	18201775-2523281	2.118	426	2450661	13.3	16.6
310.38742.186	18 20 34.835	-23 20 58.96	18203483-2320589	2.093	369	2451180	<14.6	17.2
163.27555.232	18 20 36.281	-26 26 48.06	18203628-2626480	2.021	357	2449770	13.7	16.3
311.38732.104	18 20 36.475	-24 00 20.43	18203647-2400204	2.108	375	2451210	<14.0	16.0
160.27572.1769	18 20 43.324	-25 17 33.96	18204332-2517339	1.976	291	2451290	14.9	18.7
160.27699.302	18 20 46.220	-25 28 59.84	18204622-2528598	2.069	395	2449959	12.0	15.7
142.27644.69	18 20 49.104	-29 09 37.98	18204910-2909379	1.698	311	2449901	11.7	15.1
142.27779.83	18 21 02.770	-28 49 01.10	18210276-2849011	1.734	422	2450599	13.3	16.9
153.27751.109	18 21 09.507	-30 40 26.89	18210950-3040268	1.547	360	2449567	12.8	16.0
142.27900.1700	18 21 24.929	-29 24 12.56	18212492-2924125	1.550	209	2450606	15.8	19.0
142.27906.35	18 21 28.061	-29 01 48.46	18212806-2901484	1.576	341	2449540	11.8	<15.1
142.27907.80	18 21 29.408	-28 58 17.41	18212940-2858174	2.177	416	2449592	13.3	16.5
146.27895.17	18 21 31.692	-29 46 08.71	18213169-2946087	1.649	371	2450596	13.3	<15.9
146.27899.25	18 21 36.608	-29 27 50.58	18213660-2927505	1.730	436	2450224	13.2	17.4
153.28008.17	18 21 40.503	-30 52 53.03	18214050-3052530	2.706	423	2450295	13.7	16.9
156.28515.180	18 23 07.692	-31 46 44.23	18230769-3146442	3.342	450	2449505	16.1	19.5
136.28693.40	18 23 11.439	-28 33 56.24	18231143-2833562	1.488	296	2449919	11.2	15.5
146.28675.49	18 23 17.236	-29 43 46.52	18231723-2943465	1.373	283	2449592	12.0	15.6
137.29336.35	18 24 56.017	-29 00 26.49	18245601-2900264	1.628	347	2451430	12.5	15.6
143.29457.8	18 25 11.231	-29 36 46.90	18251123-2936469	1.703	372	2450607	12.5	<15.3
143.29845.51	18 25 55.396	-29 47 26.72	18255539-2947267	1.827	408	2451334	12.4	15.7
143.30111.38	18 26 34.461	-29 21 02.14	18263446-2921021	1.401	229	2450240	11.4	15.2
143.30110.14	18 26 36.115	-29 23 54.74	18263611-2923547	1.677	472	2449462	13.0	16.0
143.30111.25	18 26 49.095	-29 22 33.65	18264909-2922336	1.358	303	2450609	12.5	16.0
132.30519.13	18 27 39.540	-28 10 52.19	18273954-2810521	1.832	477	2451303	11.7	15.2
132.30776.12	18 28 10.265	-28 20 00.39	18281026-2820003	1.505	312	2450635	11.4	15.2
138.30903.43	18 28 32.977	-28 32 07.03	18283297-2832070	2.022	381	2451260	<13.3	15.6
132.31039.35	18 28 53.158	-28 08 12.36	18285315-2808123	1.560	186	2450973	13.7	18.1
132.31298.385	18 29 21.718	-28 11 45.55	18292171-2811455	2.508	416	2450647	15.6	19.7
303.44071.416	18 29 24.623	-15 16 56.18	18292462-1516561	3.021	216	2450670	17.4	21.6
144.31804.36	18 30 33.284	-29 08 30.76	18303328-2908307	1.875	352	2449395	<13.2	15.8
303.45254.157	18 31 16.914	-14 50 22.75	18311691-1450227	2.040	403	2449789	14.3	>16.8
139.32207.1904	18 31 32.539	-28 18 10.58	18313253-2818105	3.537	500	2450230	16.7	20.4
139.32203.1597	18 31 37.023	-28 32 17.35	18313702-2832173	2.633	431	2450970	15.7	19.6
301.45610.67	18 31 50.324	-13 28 45.18	18315032-1328451	2.134	473	2451301	14.5	17.6
303.45583.155	18 32 02.377	-15 15 06.15	18320237-1515061	2.224	456	2451310	16.1	20.0
301.45778.398	18 32 02.568	-13 27 40.75	18320256-1327407	2.201	351	2451103	14.1	17.1
303.45752.231	18 32 14.204	-15 11 24.71	18321420-1511247	2.122	335	2451401	14.6	18.3
139.32728.13	18 32 40.682	-28 14 59.07	18324068-2814590	1.571	383	2451302	<11.8	15.7
139.32850.23	18 33 00.154	-28 44 01.19	18330015-2844011	1.641	396	2451302	12.0	15.2
139.32982.4362	18 33 22.698	-28 37 39.05	18332269-2837390	1.832	386	2451302	13.2	16.2
134.33253.632	18 33 57.541	-27 52 55.45	18335754-2752554	1.484	360	2449611	12.3	15.6
134.33381.3349	18 34 17.318	-27 59 44.34	18341731-2759443	1.491	357	2449541	12.1	15.6
134.33385.120	18 34 21.530	-27 46 10.28	18342152-2746102	1.798	369	2449400	<13.2	15.9

Figure 6 – Light curves (left panels) and folded light curves (right panels) of the 192 Mira variables identified in this work, based on MACHO R_C data. Data have been folded with the periods listed in Table 1.

